ZnSe based colloidal nanocrystals: synthesis, shape control, core/shell, alloy and doped systems

Peter Reiss

Received (in Montpellier, France) 6th August 2007, Accepted 20th September 2007
First published as an Advance Article on the web 1st October 2007
DOI: 10.1039/b712086a

Colloidal ZnSe nanocrystals (NCs) exhibit size-dependent fluorescence in the wavelength range of 350–450 nm, making them promising emitters for optoelectronic devices in the blue/near UV region. This *Perspective* review gives an overview of the chemical synthesis methods developed for size- and shape-controlled ZnSe NCs as well as for related core/shell and alloy structures. Special emphasis is put on the discussion of the optical and structural properties of the obtained nanostructures. Finally, the use of ZnSe as a host material for magnetic or luminescent dopant ions is highlighted.

1 Introduction

In the past two decades, zinc selenide nanostructures were the subject of intensive research as this material is considered to be—together with gallium nitride and silicon carbide—the leading candidate for the fabrication of blue light-emitting diodes (LEDs) and laser diodes (LDs).[1] Both types of devices are technologically important. Blue LEDs are building blocks of full-color electroluminescent displays and can be used for the generation of white light when combined with green and red ones or with yellow–green ones. Solid-state lighting based on LEDs is far less energy consuming than the use of traditional light bulbs. In addition, such devices have very long lifetimes of up to a few 10 000 h. Replacing the currently used red lasers (650 nm) in the field of optical data storage by blue LDs emitting at 405 nm allows for a considerable increase of the storage density of compact disks and DVDs. Next generation DVDs with a capacity of 25 GB (single layer) and 50 GB (dual layer) are currently being developed by major manufacturers under the labels of Blu-ray™ and Blu-ray Disc™ (BD).

More recently, ZnSe has also received attention of the research community dealing with chemically (“bottom-up”) synthesized colloidal nanocrystals (NCs). These nanostructures comprise an inorganic semiconductor core (ZnSe), surrounded by a corona of organic surfactants, also known as stabilizing ligands. One of the most interesting features of NCs is the dependence of their band gap on their size, originating from the quantum confinement effect. As a consequence several physical properties, which are determined by the band gap width, such as photoluminescence wavelength and others, can be precisely tuned by changing the nanocrystal size. The phenomenon of quantum confinement occurs once the diameter becomes smaller than *ca.* 9 nm, *i.e.* twice the Bohr exciton radius of ZnSe. Its practical exploitation in science and technology requires the elaboration of synthesis methods leading to quasi-monodispersed NCs.

This *Perspective* review summarizes the wet-chemical synthesis strategies for ZnSe NCs developed to date along with the structural and optical properties of the obtained samples. Core/shell systems, consisting of ZnSe and a second semiconductor material in an onion-like structure, are also discussed, with ZnSe playing the role of either the core or the shell material. In the following, alloy systems such as $Cd_{1-x}Zn_xSe$ are reviewed, which provide the possibility to tune the band gap with the composition x. Finally, results are presented concerning ZnSe NCs serving as a host material for transition metal ions, inducing new emission and/or magnetic properties. On the other hand, general considerations concerning the synthesis of monodisperse semiconductor NCs are not included in this article. The interested reader is referred to excellent recent reviews on this topic.[2]

Peter Reiss received his PhD in Inorganic Chemistry from the University of Karlsruhe in the group of Prof. D. Fenske in 2000. After a post-doctoral stay at the Atomic Energy Commission (CEA) in Grenoble, he obtained in 2002 a permanent research position in the Fundamental Research Department on Condensed Matter (DRFMC) of CEA. His scientific interests are in the field of semiconductor nanocrystals, metal nanoparticles and their molecular composites with electroactive oligomers and polymers. Dr Reiss published several papers on the synthesis, surface functionalization and assembly of nanocrystals, aiming at their application in biological labeling, optoelectronic devices and magnetic data storage media.

CEA Grenoble DSM/DRFMC/SPrAM (UMR 5819 CEA-CNRS-Université Joseph Fourier 1)/LEMOH 17 rue des Martyrs, 38054 Grenoble cedex 9, France. E-mail: peter.reiss@cea.fr

Table 1 Material's constants of bulk ZnSe.[3]

Structure (300 K)	Effective electron mass/$m_e{}^*m_0{}^{-1}$	Effective hole mass/$m_h{}^*m_0{}^{-1}$	Bohr exciton radius, r_B/nm	Exciton binding energy/meV	Optical dielectric permittivity, ε	Lattice parameter/Å	Density/ kg m^{-3}
Zinc-blende	0.157	0.935	4.5	18	8.7	5.668	5266

2 Basic material's parameters of bulk and nanocrystalline ZnSe

Cubic ZnSe has a bulk band gap $E_g{}^{bulk}$ of 2.7 eV (460 nm) at room temperature. Other material's constants are summarized in Table 1.

Fig. 1 shows the relationship between the radius r of spherical ZnSe NCs and their band gap, using the formula of Brus (eqn (1)) based on the effective mass approximation.[4]

$$E_g = E_g^{bulk} + \frac{\hbar^2\pi^2}{2r^2}\left(\frac{1}{m_e^*}+\frac{1}{m_h^*}\right) - \frac{1.8e^2}{4\pi\varepsilon\varepsilon_0}\frac{1}{r} \qquad (1)$$

The size dependence of the electronic energy levels of ZnSe NCs has been studied by photoluminescence excitation (PLE) spectroscopy and analyzed using effective mass approximation calculations.[5] The first four prominent transitions were assigned as indicated in Fig. 2.

Most binary octet semiconductors crystallize either in the cubic zinc-blende (ZB) or in the hexagonal wurtzite (W) structure, both of which vary in the layer stacking along (111), showing an ABCABC or an ABAB sequence, respectively. The low-temperature ground state structure of ZnSe is ZB. However, due to a relatively low difference in the total energy between the ZB and the W structure (5.3 meV atom^{-1}),[6] ZnSe exhibits the so-called W–ZB polytypism. Depending on the experimental conditions, nucleation and growth of the NCs can take place in either structure and also the coexistence of both structures in the same nanoparticle is possible.

3 The chemical synthesis of ZnSe NCs

In this section, the description of the current state of the art is divided into a small number of synthetic approaches, which are illustrated by highlighting some representative articles in more detail. As a matter of fact, essentially all methods for the preparation of ZnSe NCs were derived from those initially developed for cadmium chalcogenides NCs. Table 2 gives an overview of the most widely applied synthesis methods and of the characteristics of the resulting ZnSe NCs.

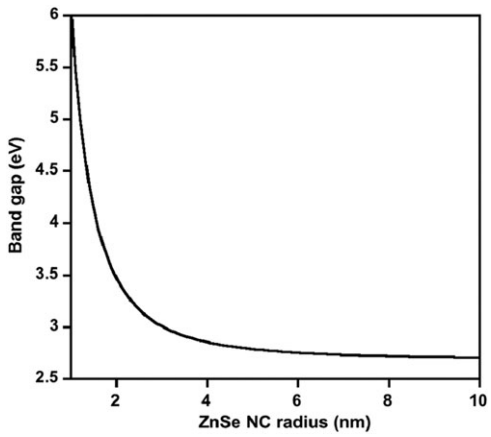

Fig. 1 Correlation between the size of ZnSe NCs and their band gap.

3.1 Arrested precipitation

Brus and coworkers were the first to report the synthesis of colloidal ZnSe NCs using the technique of *arrested precipitation*.[7] In this approach, small crystallites were produced by the reaction of Zn and Se precursors at low temperature (−80 °C) in 2-propanol or at room temperature in methanol or in an ethylene glycol–water mixture. Thermal coagulation and Ostwald ripening could be controlled by carrying out the synthesis at low temperature, and *via* the repulsion of individual crystallites by adsorption of stabilizing solvent molecules. The prepared NCs showed distinct features of the quantum confinement. In particular, the onset of their optical absorption was hypsochromically shifted with respect to the case of the bulk crystals. Moreover, characteristic excitonic features could be detected at 290, 320 and 390 nm in the absorption spectra depending on the size of the prepared crystallites. Unfortunately, no information concerning the photoluminescence (PL) properties of these samples was given, and the crystallites exhibited a strong tendency to aggregate, as no stabilizing ligands were present in the reaction medium.

3.2 Precipitation in presence of stabilizers

An important synthetic approach, which has also been successfully applied to other materials and in particular to

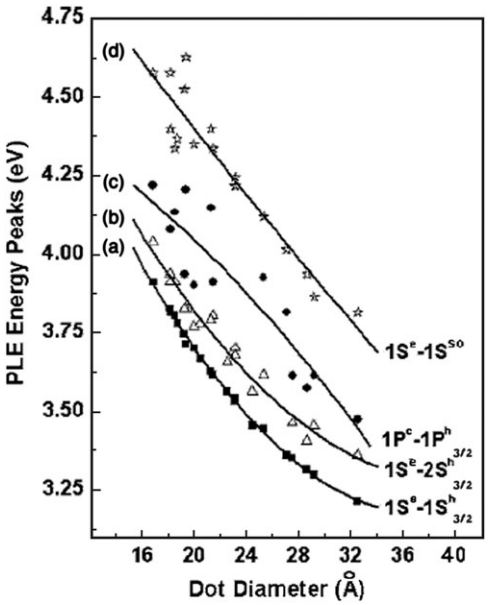

Fig. 2 PLE peak energies for different transition states as a function of the size of ZnSe NCs. Reprinted with permission from ref. 5. Copyright 2006, American Institute of Physics.

Table 2 Chemical synthesis methods for ZnSe NCs and selected sample properties (n.g.: not given in the article)

Method	Zn precursor	Se precursor	Solvent	Stabilizing ligands	Temp. injection/ growth (°C)	Size/ nm	Crystal structure	PL wavelength/ nm	FWHM/ nm	Ref.
AP[a]	$Zn(ClO_4)_2$	H_2Se	MeOH or *i*-PrOH	—	−80 or RT	n.g.	ZB	n.g.	n.g.	7
Pstab[b]	$Zn(ClO_4)_2$	H_2Se	H_2O	TG, TGA, MPA	RT/100	2–3	ZB	375	n.g.	8
Pstab[b]	$ZnCl_2$	NaHSe	H_2O	MPA	140 (micro-wave)	2.3–3.4	ZB	400	n.g.	9
RM[c]	$Zn(ClO_4)_2$	Na_2Se	Heptane–H_2O–AOT	Mercaptododecanol	RT	3.4	ZB	355	>50	10
HI[d]	$EtZnSe_2CNEt_2$		TOPO–TOP	TOPO/TOP	250/250	4.9	W	446	>50	11
HI[d]	$Zn(SePh)_2 \cdot TMEDA$		TOPO–TOP	TOPO/TOP	320–385	2.7–4.9	ZB	387–451	n.g.	12
HI[d]	Et_2Zn	TOPSe	HDA	TOP/HDA	310/270	4.3, 6	ZB	365–445	n.g.	13
HI[d]	Zinc stearate	TOPSe	Octadecane	Stearate/TOP	250 or 300	3–7	W	390–440	12–17	14
HI[d]	ZnO	TOPSe	HDA	Laureate/ HDA/TOP	300/280	2.5–6	W	400–440	n.g.	15
HU[e]	$[Zn_{10}Se_4(SPh)_{16}]^{4-}$		HDA	SPh/HDA	220–280	2–5	ZB	380–410	18–22	16
HU[e]	$ZnCl_2$	Se powder or $NaSeO_3$/ hydrazine	EtOH–H_2O or glycol, octanol–H_2O	Linoleic acid/ sodium linoleate	140–180	6–8	n.g.	n.g.	n.g.	17

[a] Arrested precipitation. [b] Precipitation in presence of stabilizers. [c] Reverse-micelles method. [d] Hot-injection method. [e] Heating-up method.

CdTe, is the *precipitation in the presence of stabilizers* using water as a solvent. While the precursors remain the same as in the synthesis *via arrested precipitation*, the resulting NCs are stable at room temperature since the stabilizing ligands prevent them from aggregation. Several thiol containing stabilizing molecules have been applied (thioglycerol, TG; thioglycolic acid, TGA; 3-mercaptopropionic acid, MPA).[8] The reaction is triggered by bubbling H_2Se gas through the aqueous solution of the zinc salt and the stabilizer, followed by refluxing the reaction mixture for several hours to accomplish NCs' growth. Optimal pH values for the formation of stable colloids were found to be 11.5 in the case of TG stabilizing molecules and 6.5 when TGA or MPA were used. The photoluminescence quantum yield (PL QY) of the obtained NCs increases from less than 0.1% to 10–30% by the irradiation with white light during several hours. The irradiation process, in addition to improving the PL QY, produced a bathochromic shift of the NCs' excitonic peak. Both phenomena resulted from the photochemically induced incorporation of sulfur, originating from the TGA stabilizer, into the crystal lattice to give better passivated $ZnSe_{1-x}S_x$ alloyed NCs.

A derived method using microwave irradiation resulted in a significant shortening of the NCs preparation procedure.[9] Similarly as in the previously discussed case, the relatively high value of the PL QY (17%) was attributed to the microwave induced decomposition of the MPA stabilizer and subsequent formation of a ZnSe(S) alloy shell on the surface of the ZnSe NCs. Another modification of the original method[8] was reported by Murase and co-workers, who focused on the optimization of the irradiation conditions. UV irradiation (365 nm) was used instead of white light, better matching the absorption spectrum of the ZnSe NCs. Consequently, the irradiation time could be reduced to less than 2 h before reaching the maximum PL intensity. The resulting NCs showed a tunable emission in the spectral range of 405–435 nm with a PL QY up to 50%.[18]

3.3 Synthesis in reverse micelles

Both *reverse micelles*, *i.e.* nanometer-sized droplets of water in oil stabilized by amphiphilic molecules, and more recently *normal micelles* (stabilized oil nanodroplets in water) have successfully been applied as soft templates or microreactors for the synthesis of a large variety of semiconductor NCs, metal and oxide nanoparticles.[19] Although versatile in its nature, this method has not been extensively used for the preparation of ZnSe NCs. One of the scarce examples is the report of Quinlan *et al.* who obtained with the reverse micelles approach 3.4 nm NCs exhibiting a broad emission peak with a maximum at 355 nm.[10] In the case of cadmium chalcogenide NCs, it has been observed that the maximum achievable size with this technique is around 4 nm, which—in view of the similar reaction conditions—could be an upper limit also for ZnSe NCs.[19a] Furthermore, Pileni and coworkers demonstrated that when reverse micelles are used as nanoreactors for NC growth, the final particle size is not the same as that of the droplet used as a template. This "discrepancy" may constitute an intrinsic limitation for the precise size (and shape) control of NCs prepared by this method.[19a,c] A different reverse micellar type of soft template, namely lyotropic liquid crystals, formed by the self-assembly of an amphiphilic block copolymer (poly(ethylene oxide)–poly(propylene oxide)–poly(ethylene oxide)) in a water–*p*-xylene mixture, was applied for both size and shape control of ZnSe NCs.[20] Using zinc acetate and gaseous H_2Se precursors, approximately 3 nm sized ZnSe NCs were obtained and the method was further extended to the synthesis of ZnSe hollow spheres, nanotubes and plate-like structures.

3.4 Hot-injection method

The *hot-injection method* is aiming at a temporal separation of the NCs nucleation and growth processes *via* creation of a nucleation burst by rapid injection of precursors into a hot solvent. During this nucleation process the monomer supersaturation decreases below the nucleation threshold and in the subsequent reaction stage the formed seeds homogeneously grow to NCs. A recent review focuses on the potential of this approach for the preparation of monodispersed NCs.[21] The *hot-injection method* was first developed for the synthesis of cadmium chalcogenide NCs, with trioctylphosphine (TOP) as

the chalcogenide precursor solubilizing agent and trioctylphosphine oxide (TOPO) acting at the same time as the solvent and as the stabilizing ligand.[22] In early works, aimed at the preparation of ZnSe, the same solvent/ligand couple was applied. For example, the use of a monomolecular precursor, ethyl(diethyldiselenocarbamato)zinc, dissolved in TOP and injected into hot TOPO, resulted in NCs exhibiting a rather broad emission centered at 446 nm.[11] In a similar procedure, the air-stable complex bis(phenylselenolato)zinc–tetramethylethylenediamine (TMEDA) gave rise, depending on the growth temperature, to ZnSe NC of different size and low size dispersion, exhibiting emission wavelengths in the range of 387–451 nm.[12]

Hines and Guyot-Sionnest reported the synthesis of ZnSe NCs showing strong band edge emission in the range from 365–445 nm with PL QYs of 20–50%.[13] Adapting the work on CdSe NCs by Murray *et al.*,[22] they used an organometallic zinc precursor (diethylzinc) and selenium powder dissolved in TOP (TOPSe). The major difference, with respect to the case of CdSe was the use of hexadecylamine (HDA) as a solvent. TOPO turned out to bind too strongly to Zn and therefore an appropriate balance between the nucleation and the growth crucial for good size control could not be achieved. At the same time, the combination of HDA and TOP efficiently passivated the NCs' surface by removing trap states/dangling bonds, which resulted in pure band edge fluorescence.

Most probably one of the simplest methods for the preparation of a size series of ZnSe NCs was reported in 2004 by our group.[14] Here, pyrophoric diethylzinc was replaced by an air-stable and easy to manipulate precursor (zinc stearate), while keeping the established Se precursor (TOPSe). In the growing process zinc stearate served not only as the cation precursor but also as a source of stabilizing stearate ligands. The size of the obtained ZnSe could be varied from 3 to 7 nm by adjusting the concentration of the zinc precursor in the reaction mixture and/or varying the temperature, and the resulting absorption and PL spectra are depicted in Fig. 3.

Coordinating solvents, such as TOPO or HDA, having usually the double function of the reaction medium *and* the stabilizing ligand in traditional *hot-injection methods*, were replaced by a simple long-chain alkane, namely octadecane. The use of a similar non-coordinating solvent, 1-octadecene, was first proposed by Yu and Peng in the preparation of cadmium chalcogenides NCs.[23] In the case of octadecane, the absence of the double bond within the alkyl chain eliminates the possibility of a direct implication of the solvent in the reaction pathway and simplifies the investigation of the reaction mechanism. Based on recent NMR spectroscopic studies,[24] the following reaction pathway of the formation of ZnSe from zinc stearate and TOPSe can be postulated (see Scheme 1):

In the proposed mechanism, Zn–Se formation occurs *via* the activation of TOPSe by a Lewis acidic zinc center to the nucleophilic attack of a carboxylate ion, resulting in the cleavage of the P=Se bond and the formation of a P=O bond in a substitution reaction.[24] Consequently, the reaction side products *i.e. in situ* generated trioctylphosphine oxide (TOPO) and stearic acid anhydride are supposed to bind to the

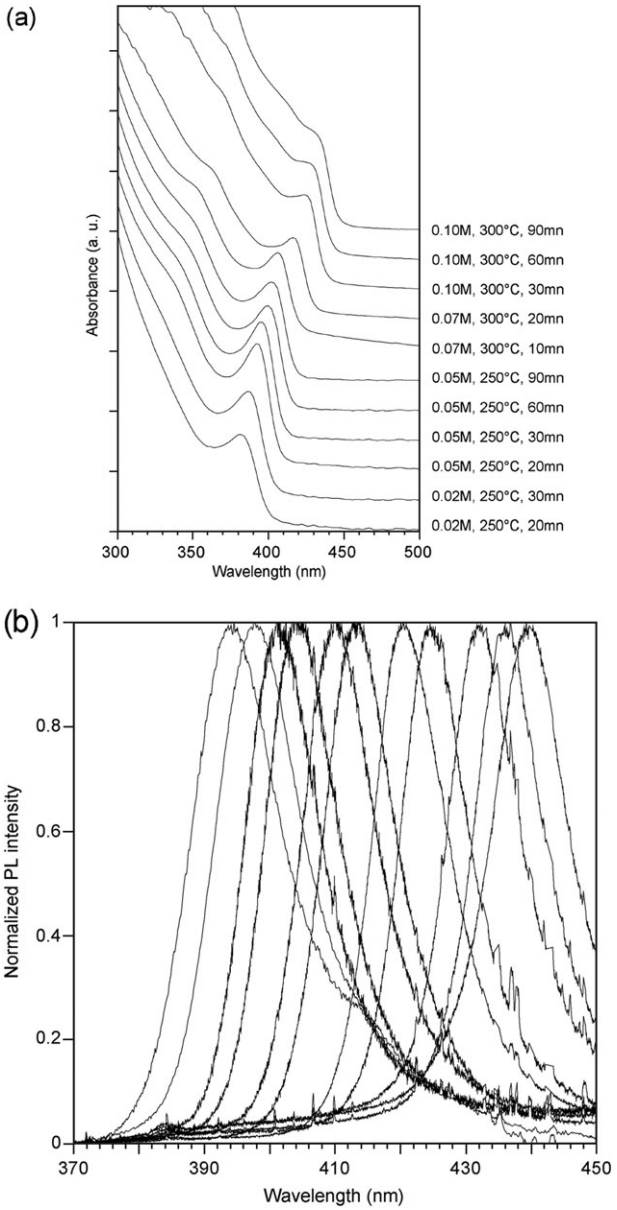

Fig. 3 Absorption (a) and PL (b) spectra of a size series of ZnSe NCs prepared by the *hot-injection method* using the non-coordinating solvent octadecane. Reprinted with permission from ref. 14. Copyright 2004, Elsevier.

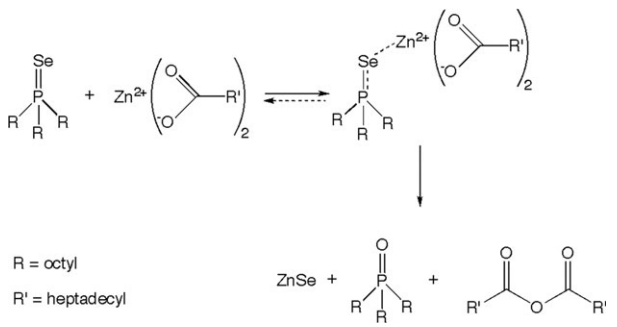

Scheme 1 Proposed reaction pathway for the formation of ZnSe NCs from zinc carboxylate and TOPSe precursors.

NC surface more likely than initially used stearate and/or TOP ligands.

Li *et al.* reported a similar route implying the use of a mixture of 1-octadecene and tetracosane combined with the addition of a small amount of octadecylamine (ODA) to the reaction mixture.[25] According to these authors, ODA was necessary to activate the zinc carboxylate precursor, otherwise no NCs with low size distributions could be obtained. Finally, Chen *et al.* used a shorter chain zinc carboxylate, namely zinc laurate generated *in situ* from ZnO and lauric acid in HDA. Size control of the obtained ZnSe NCs was achieved in a range of 2.5–6 nm by varying the reaction time.[15]

3.5 Heating-up method

The *heating-up method* consists of the mixing of all precursors and stabilizers in the solvent at room temperature or moderately elevated temperature, followed by the rapid heating of the flask to the temperature appropriate for NC growth. This approach, which can easily be scaled up due to the absence of the pyrolytic event characterizing the *hot-injection method*, has been widely applied in the synthesis of metal and oxide nanoparticles.[26] Cumberland *et al.* used air-stable $[Zn_{10}Se_4(SPh)_{16}]^{4-}$-clusters as monomolecular precursor for the synthesis of 2–5 nm ZnSe NCs in HDA, controlling the size with the reaction temperature (220–280 °C).[16] More recently, Li's group reported a related, very general approach for the synthesis of a large variety of nanoparticles including metals, oxides, and semiconductors, exhibiting low size dispersions.[17] The strategy is based on the phase transfer and separation mechanism occurring at the interfaces of the liquid, solid and solution phases present during the synthesis and is also referred to *interface-mediated growth* or *LSS approach*. The detailed description of the underlying mechanism goes beyond the scope of this review and the interested reader is referred to the original literature.[17] Sharp size distributions have been obtained in particular with noble metal, transition metal sulfide and fluoride nanoparticles. In the case of ZnSe NCs, the method yields 6–8 nm particles depending on the reaction temperature (140–180 °C) with a size distribution of 10–15% and TEM images of the samples reveal a distribution of shapes (spherical, rice shaped, oval). Both selenium powder or a $NaSeO_3$/hydrazine mixture can be applied as the Se source, which is mixed with a water-soluble Zn salt and fatty acid type stabilizing compounds in an ethanol–water mixture and subsequently heated in an autoclave. In an extension of this approach, the same group synthesized 2 μm sized ZnSe hollow microspheres constituted of small 5–6 nm NCs.[27]

4 Shape control of ZnSe NCs

As illustrated by the experimental data discussed above, depending on the reaction conditions, ZnSe NCs exhibit either zinc-blende (ZB) or wurtzite (W) structure. This polytypism is very useful for the generation of NCs exhibiting anisotropic shapes (rod-like or branched (bipod, tripod, tetrapod, multipod)). An illustrative example of the application of colloidal chemistry in this field was the synthesis of CdSe and CdTe tetrapods of controlled arm length and diameter.[28] Cozzoli *et al.* identified experimental conditions for the preparation of ZnSe NCs of various shapes: spheres, rods, and three-dimensional structures comprising rods interconnected by branching points.[29] In a modification of the organometallic *hot-injection* approach, diethylzinc and TOPSe or TBPSe (tributylphosphine selenide) precursors were used in combination with the coordinating solvents HDA or ODA. The rate of precursor addition played a decisive role in the shape evolution of the ZnSe NCs. High injection rates yielded spherical NCs of ZB structure. The size of these particles could be adjusted by varying the chain length of the used amine or by changing the injection/growth temperature. However, the ZB structure, being more symmetric than the W one, does not have a single preferential growth direction. On the other hand, it was found that very low monomer concentrations, achieved by low precursor injection rates, promoted the W structure, which then induced anisotropic NC growth along the unique *c*-axis. Furthermore, the experimental results indicated that the alkylamine molecules stabilized the facets of W ZnSe NCs more efficiently than the facets of the ZB ones in near-equilibrium conditions. Consequently the combination of low supersaturation and high temperature (345 °C) provided thermodynamic control of the growth mode and enabled the switching between the ZB and W structures. As the difference in the total energy between the ZB and the W structure is relatively low (see Section 2),[6] such an alternation could however also occur in an uncontrolled manner during growth, giving rise to curvature of the obtained nanorods or to multiple branching points. Thermochemical methods based on evaporation and condensation vapor processes provide—at least to date—a higher degree of shape selectivity for ZnSe nanostructures as compared to solution chemical methods.[30] An exception is the following example: in the continuity of their previous work on anisotropic ZnS nanostructures,[31] Efrima and co-workers

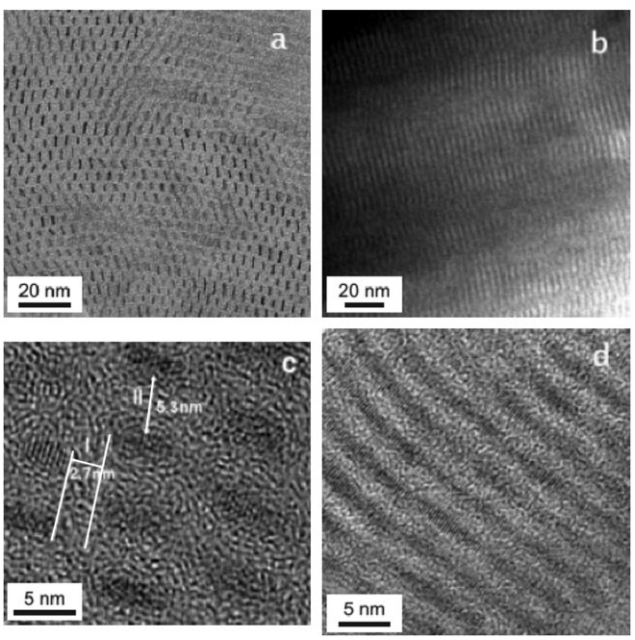

Fig. 4 TEM images of ZnSe nanorods (a, b) and nanowires (c, d). Reproduced with permission from ref. 32. Copyright 2005, Wiley-VCH Verlag GmbH & Co. KGaA.

developed the synthesis of very thin ZnSe nanorods (1.3 × 4.5 nm) and nanowires (1.3 × 100–200 nm) of uniform length, which spontaneously self-assemble into highly ordered 2D superstructures (Fig. 4).[32]

Synthesis was carried out at significantly lower temperatures than in typical *hot-injection* NC preparations (140 °C) and proceeded by adding a mixture of selenourea, dimethylformamide and molten ODA to a solution of zinc acetate in molten ODA. At short reaction times (20–25 min), ZnSe nanorods were formed, longer times (*ca.* 1 h) provided nanowires, both showing W structure. In analogy with the case of ZnS nanostructures,[31] a synchronous oriented end-to-end attachment mechanism occurring in ordered phases of nanorods has been postulated to explain the observed rod-to-wire transition.

In contrast to the approach of Cozzoli *et al.* presented above,[29] where NC synthesis took place in the diffusion-controlled growth regime, here anisotropic NC growth was achieved in the reaction-controlled growth mode.[33] The NC shape is determined by the difference in growth rate of the individual crystal facets. ODA preferentially binds to the Zn (and not to the Se) atoms at the NCs' surface and the adsorption of ODA molecules occurs with a significantly slower kinetics than ZnSe growth. TEM analysis of the interparticle spacing in ordered nanorod arrays (Fig. 4(c)) indicated that the lateral facets as well as one end of the growing nanorods were covered with ODA molecules, leading to one-dimensional growth from the other end.

5 Core/shell structures involving ZnSe

Depending on the band gap and the relative position of electronic energy levels of the involved semiconductors, the shell can have different functions in core/shell (CS) NCs. Scheme 2 gives an overview of the band alignment of selected bulk materials. Two main cases can be distinguished, denominated type I and type II band alignment, respectively. In the former, the band gap of the shell material is larger than that of the core one, and both electrons and holes are confined in the core. In the latter, either the valence band edge or the conduction band edge of the shell material is located in the band gap of the core. The resulting staggered band alignment leads upon excitation of the NC to a spatial separation of the hole and the electron in different regions of the CS structure.

In type I CS NCs, the shell is used to "passivate" the surface of the core with the goal to improve its optical properties. The shell separates physically the surface of the optically active core NC from its surrounding medium. As a consequence, the sensitivity of the optical properties to changes in the local environment of the NCs' surface, induced for example by the presence of oxygen or water, is reduced. With respect to core NCs, CS systems generally exhibit enhanced stability against photo-degradation. At the same time, shell growth reduces the number of surface dangling bonds, which can act as trap states for charge carriers and reduce the PL QY. In type II systems, the staggered band alignment leads to a smaller effective band gap than each one of the constituting core and shell materials. The interest of these systems is the possibility to tune the emission colour with the shell thickness towards spectral ranges, which are difficult to attain with other materials.

ZnSe has been overcoated with ZnS using organometallic precursors, leading to an emission wavelength centered at 400 nm (FWHM 20 nm) and a PL QY of 17%.[35] In a newer, one-pot approach based on the use of alternative precursors (zinc laurate and TOPS), shell growth was carried out at 180 °C in HDA and QYs up to 30% were reached.[36] Nevertheless QYs superior to 50%, routinely obtained for cadmium-based CS NCs, have not yet been achieved with ZnSe cores, pointing at the fact that ZnS, providing a relatively low conduction band offset, is probably not the best choice as the shell material.

Klimov and co-workers studied the optical properties of so-called "inverted" CS NCs, *i.e.* the band gap of the core material (ZnSe) was larger than that of the shell material (CdSe).[37] On the basis of the radiative recombination lifetimes recorded for NCs with a fixed core size and increasing shell thickness, a continuous transition from type-I to type-II and back to type-I localization regimes was observed. Thin CdSe shells ($d < 1.1$ nm) do not provide any electron or hole shell-localized states and the ground state energies lie above the band edge of ZnSe. Consequently both electron and hole wave functions are distributed over the entire NC. In the case of a rather thick CdSe shell ($d > 1.6$ nm), the ground conduction and valence band states are below the ZnSe band edge, resulting in the localization of both electron and hole in the shell. This situation corresponds to the band alignment of both materials represented in Scheme 2. For intermediate shell thicknesses, the carriers are spatially separated between the shell (electron) and the core (hole). The samples exhibited emission in the range of 430–600 nm and QYs of 60–80%. The same CS system was also synthesized applying CdO dissolved with oleic acid in octadecene and TOPSe as the shell precursors instead of dimethylcadmium/TOPSe.[38] By varying the CdSe shell thickness on 2.8 core ZnSe NCs (Fig. 5), the emission wavelength could be tuned in a broad spectral range (417–678 nm) with QYs of 40–85%.

ZnSe can also be an interesting shell material in core/shell structures, as shown by our group in the case of CdSe/ZnSe NCs. In this system, the electrons are efficiently confined in the NC core due to the large conduction band offset, while only a relatively small barrier exists for the holes. In spite of the relatively large lattice mismatch of 6.9% between CdSe and

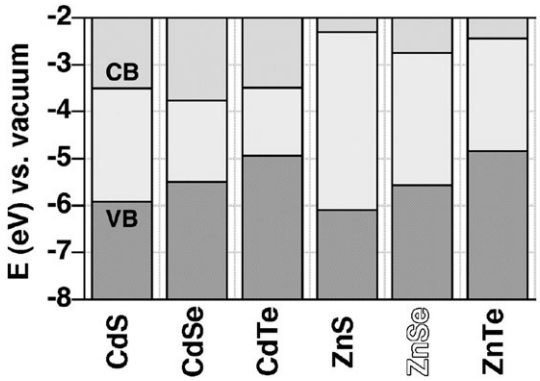

Scheme 2 Electronic energy levels of selected bulk semiconductors (VB: valence band, CB: conduction band). Valence band offsets from ref. 34.

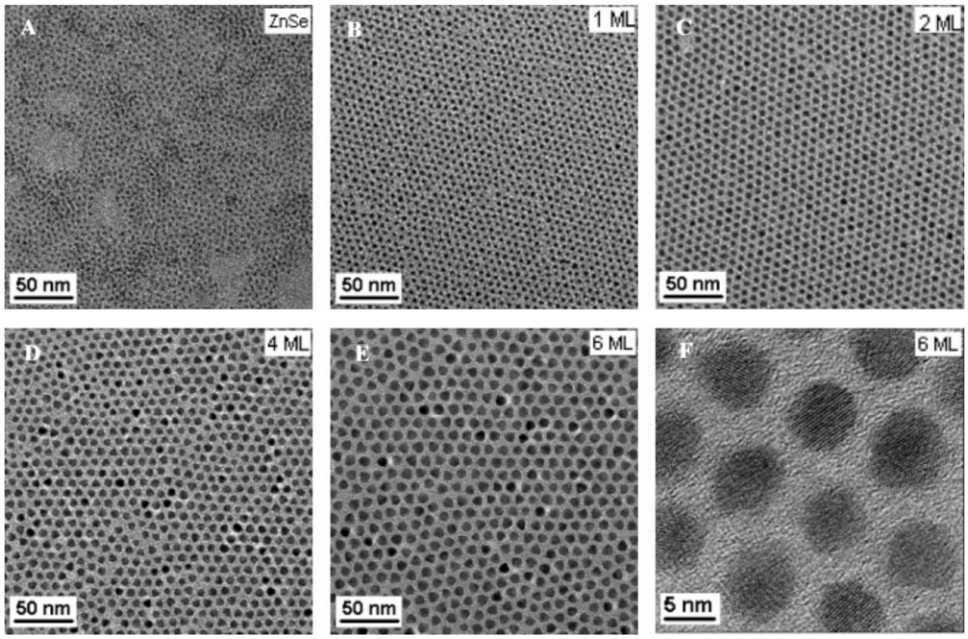

Fig. 5 TEM images of ZnSe NCs and corresponding ZnSe/CdSe core/shell NCs. The shell thickness is indicated with the number of monolayers (ML). Reprinted with permission from ref. 38. Copyright 2005, American Chemical Society.

ZnSe, the common anion structure is favourable for epitaxial type shell growth. The obtained core/shell NCs exhibited QYs ranging from 60 to 85% and narrow emission linewidths.[39] Lee *et al*. studied the effect of lattice distortion in the CdSe/ZnSe CS system on its optical spectra by varying the concentration of the ZnSe precursor solution used for the shell growth[40] as well as the ripening kinetics upon thermal annealing.[41] Finally, ZnSe has been used as "lattice-adapting" interlayer in core/shell/shell (CSS) structures comprising a CdSe core and a ZnS outer shell.[42] In these systems, the intercalated ZnSe shell reduces the number of strain induced defects between the core and the outer shell material, which exhibit a large lattice mismatch of *ca.* 10%. CSS structures generally exhibit superior optical properties and stability with respect to CS systems.[43]

6 Alloy NCs comprising ZnSe

As demonstrated in Section 3, by taking advantage of the quantum confinement effect it is possible to tune, through size control, the fluorescence wavelength of ZnSe NCs from the blue to the near UV spectral range. The formation of an alloy structure is an alternative way to influence the band gap of the NCs, not by changing their *size* but their *composition*. A typical example are $Cd_{1-x}Zn_xSe$ NCs where a fraction of the Zn atoms are substituted by Cd atoms in the crystal lattice. The band gap of the resulting ternary alloy is in between those of pure ZnSe and of pure CdSe NCs of the same size. In contrast to the crystal lattice parameters, which show, according to Végard's law, a linear evolution with composition, the curve describing the corresponding evolution of the band gap shows a deviation from linear behavior. However, as can be seen from Fig. 6, this difference is not very pronounced for the common anion system $Cd_{1-x}Zn_xSe$.[44] A measure of this deviation is the so-called bowing parameter, which depends on the difference in electronegativity of the two end components, here CdSe and ZnSe.[45] Consequently, common cation alloys ($CdS_{1-x}Se_x$,[46] $CdSe_{1-x}Te_x$[47]) generally present larger bowing parameters than common anion ones.

Different methods of the $Cd_{1-x}Zn_xSe$ NCs synthesis were developed, deriving directly from those used for the binary compounds. While the Se precursor was generally TOPSe, the use of different Cd and Zn precursors has been explored. Organometallic approaches based on dimethylcadmium and diethylzinc were first applied[49] before the very recent

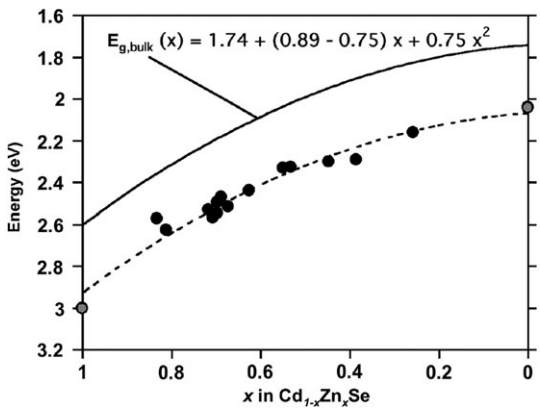

Fig. 6 Excitonic band gap *vs.* composition of 4.3 nm $Cd_{1-x}Zn_xSe$ nanocrystals. The experimental data can be fitted (dashed line) with the same parameters as the empirical function established for the evolution of the bulk band gap with composition (solid line)[48] when the energy value of bulk CdSe (1.74 eV) is replaced by the value corresponding to 4.3 nm nanocrystals (2.06 eV). Reproduced with permission from ref. 44. Copyright 2007, Wiley-VCH Verlag GmbH & Co. KGaA.

Table 3 Synthesis methods for $Cd_{1-x}Zn_xSe$ NCs and selected properties of the obtained samples

Cd precursor	Zn precursor	Se precursor	Solvent	Reaction time	PL range/nm	FWHM/nm	Ref.
Me_2Cd	Et_2Zn	TOPSe	TOPO–HDA	15 min–12 h	440–550	24–32	49*a*
Me_2Cd	Et_2Zn	TOPSe	(1) HDA (2) TOPO	90 min (ZnSe) +46 h	413–506	30–35	49*b*
Cd-stearate	Zn-stearate	TOPSe	1-Octadecene	20 min	470–580	28–35	44

development of a method in which only air-stable precursors (cadmium stearate and zinc stearate) were used.[44] The synthetic details as well as the properties of the obtained NCs are summarized in Table 3.

7 Doped ZnSe NCs

Doping—the introduction of a small amount of "impurities" into the crystal lattice—is an interesting way to change the NCs' physical properties. An important example is the doping of II–VI semiconductors with paramagnetic Mn^{2+} ions (S = 5/2), yielding materials denominated *dilute magnetic semiconductors* (DMS), which exhibit interesting magnetic and magnetooptical properties.[50] At the same time, the host NC can act as an antenna for the absorption of energy (*e.g.* light) and excitation of the dopant ions *via* energy transfer. Bulk Mn-doped ZnSe (ZnSe:Mn) exhibits photoluminescence at 582 nm (2.13 eV), commonly assigned to an optically forbidden d–d transition of Mn^{2+} ($^4T_1$ to $^6A_1$).[51] This emission is sensitive to the crystal field splitting being itself dependent on the local chemical environment.

A general problem encountered in essentially all attempts of NCs doping is the fact that the host matrix tends to expel the dopant ions to the surface, in some sort of "self-purification" process. Therefore, even in the favorable case of dopant ions, having the same valence state and similar ionic radius as the corresponding host ions, successful (volume) doping is difficult to achieve in a straightforward approach by simply adding a small amount of dopant precursor during the synthesis of the host NCs. Nevertheless, by adding dimethylmanganese[52] or manganese cyclohexanebutyrate[53] to the zinc precursor in the organometallic ZnSe synthesis,[13] successful Mn-doping has been achieved, even though some residual blue emission from the ZnSe host matrix at low dopant concentrations indicated the co-existence of both doped and undoped NCs. Similarly, the injection of TBPSe into a solution of Zn and Co acetate in a mixture of ODE, HDA and oleic acid at 310 °C led to the formation of Co^{2+}-doped ZnSe NCs.[54] However, the obtained DMS NCs contained no dopant ions in the central cores and therefore exhibited excitonic Zeeman splitting energies significantly (40%) smaller than expected from the bulk ZnSe:Co data.

A decisive step towards the understanding of the doping process was achieved by Erwin *et al.*[55] They introduced a model of doping based on kinetics and concluded that the doping mechanism is controlled by the initial adsorption of impurities on the surface of growing NCs. Only impurities remaining adsorbed on the surface for a time comparable to the reciprocal growth rate are incorporated into the NC. Three main factors influencing this residence time were determined, namely the surface morphology, NC shape and surfactants present in the growth solution. It has been shown that (001) surfaces of ZB crystals exhibit much higher impurity binding energies than the other two ZB orientations and than any facet of crystals with W or rock-salt (RS) structures. These findings were fully corroborated by the state-of-the-art, as all NCs successfully doped with Mn ions exhibited the ZB crystal structure.

A new approach with the goal to achieve the doping of *all* NCs in a given sample was explored by Peng and co-workers. In the so-called *nucleation-doping* strategy, MnSe nuclei, formed from manganese stearate and TBPSe in octadecylamine at 280 °C, were overcoated with ZnSe using zinc stearate or zinc undecylenate. No residual ZnSe emission was observed and the doped NCs exhibited thermally stable (up to 300 °C) highly efficient (QY 40–70%) PL in a spectral window of 545–610 nm, depending on the ZnSe shell thickness and on the nature of the surface ligands (charged or neutral).[56] The same approach was extended to the doping of ZnSe with Cu ions (Fig. 7).[57] In conclusion, with exception of the comparably broad PL peaks (>50 nm at FWHM), their

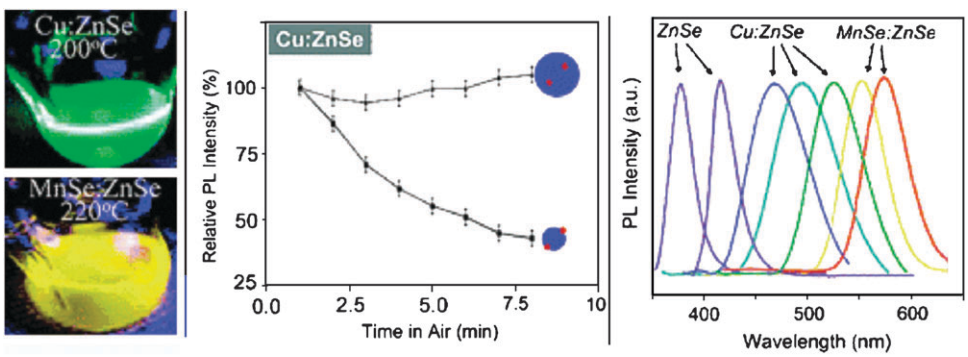

Fig. 7 Photoluminescence of Cu- and Mn-doped ZnSe NCs at high temperature (left); stability of Cu-doped ZnSe NCs in air (middle); PL spectra of ZnSe-based doped NCs (right). Reprinted with permission from ref. 57. Copyright 2005, American Chemical Society.

otherwise very interesting optical properties make transition metal doped ZnSe NCs promising "green" alternatives to the widely studied II–VI semiconductor NCs for a number of applications including biological labeling.[58]

8 Perspectives

As highlighted in this article, ZnSe plays an important role in the research devoted to semiconductor NCs. Several powerful chemical synthesis methods have been developed within the last decade, enabling the reproducible synthesis of monodisperse samples. The size dependent emission in the near UV/blue spectral range of ZnSe NCs can potentially be exploited in light emitting diodes or quantum dot lasers. Prior to this, however, surface passivation methods have to be developed to push the room temperature QY to values routinely achieved with Cd-based systems, *i.e.* beyond 50%. Another important issue to be addressed in LEDs based on 0D quantum dots is the charge injection, which is currently a bottleneck for device efficiency. This problem is circumvented in optically pumped down-conversion devices, in which ZnSe NCs can be excited with a UV diode to obtain blue emission. 1D ZnSe nanorods or nanowires supposedly provide significant advantages for the integration in optoelectronic devices. Physical methods such as VLS or MBE growth are more powerful in this respect, as they give the possibility to easily modulate the composition of nanowires in both the longitudinal and transversal axis. In this manner heterostructures comprising p–n junctions and nanowires of core/shell type can be prepared. Nevertheless, as shown in some examples in this article, also recent chemical methods allow for the shape control of ZnSe NCs, giving access not only to 1D structures but also to branched ones (tripods, tetrapods, *etc.*), which in addition can easily be manipulated in solvents due to their colloidal character. Such anisotropic ZnSe NCs are ready for use in combination with electron donors (*e.g.* conjugated polymers) in hybrid photovoltaic devices in a similar manner as other II–VI semiconductors. In the case of cadmium chalcogenides, for example, both rodlike and branched nanostructures have proven to yield superior conversion efficiencies as compared to spherical ones due to improved charge percolation to the electrode.[59] On the other hand, it still remains a synthetic challenge to obtain with solution chemistry the same degree of shape selectivity and monodispersity for ZnSe as compared to CdSe or CdTe.

Beside their use as functional building blocks for next generation optoelectronic devices, other important applications of semiconductor NCs comprise biological labels or sensors. Cadmium-based NCs, although in the center of academic research for the last 15 years, clearly do not respond to the technological and environmental needs of the future. Nanocrystalline ZnSe is one of the promising materials to close this gap, not only as a tunable blue emitter, but also, as shown, as an interesting host material for divalent transition metal ions, giving access to new optical and magnetic properties. In this context, Mn^{2+}- or Co^{2+}-doped ZnSe NCs are, similar to doped ZnO,[60] promising nanostructures for applications in the emerging field of spintronics.

Acknowledgements

The author thanks Profs. Adam Pron, Nguyen Quang Liem (VAST/IMS at Hanoi, Vietnam) and Dr Joël Bleuse for helpful discussions.

References

1 D. A. Gaul and W. S. Rees Jr, *Adv. Mater.*, 2000, **12**, 935–946.
2 (*a*) A. L. Rogach, D. V. Talapin, E. V. Shevchenko, A. Kornowski, M. Haase and H. Weller, *Adv. Funct. Mater.*, 2002, **12**, 653–664; (*b*) J. Park, J. Joo, S. G. Kwon, Y. Jang and T. Hyeon, *Angew. Chem., Int. Ed.*, 2007, **46**, 4630–4660.
3 Landolt–Börnstein, *Numerical Data and Functional Relationships in Science and Technology, New Series, Group III: Crystal and Solid State Physics*, ed. O. Madelung, M. Schulz and H. Weiss, Springer, Berlin, 1982, vol. III/17b.
4 L. E. Brus, *J. Chem. Phys.*, 1984, **80**, 4403–4409.
5 V. V. Nikesh, A. D. Lad, S. Kimura, S. Nozaki and S. Mahamuni, *J. Appl. Phys.*, 2006, **100**, 113520.
6 C.-Y. Yeh, Z. W. Lu, S. Froyen and A. Zunger, *Phys. Rev. B*, 1992, **46**, 10086–10097.
7 N. Chestnoy, R. Hull and L. E. Brus, *J. Chem. Phys.*, 1986, **85**, 2237–2242.
8 A. Shavel, N. Gaponik and A. Eychmüller, *J. Phys. Chem. B*, 2004, **108**, 5905–5908.
9 H. Qian, Z. Qiu, L. Li and J. Ren, *J. Phys. Chem. B*, 2006, **110**, 9034–9040.
10 F. T. Quinlan, J. Kuther, W. Tremel, W. Knoll, S. Risbud and P. Stroeve, *Langmuir*, 2000, **16**, 4049–4051.
11 N. Revaprasadu, M. A. Malik, M. M. Zulu, P. O'Brien and G. Wakefield, *J. Mater. Chem.*, 1998, **8**, 1885–1888.
12 Y.-W. Jun, J.-E. Koo and J. Cheon, *Chem. Commun.*, 2000, 1243–1244.
13 M. A. Hines and P. Guyot-Sionnest, *J. Phys. Chem. B*, 1998, **102**, 3655–3657.
14 P. Reiss, G. Quemard, S. Carayon, J. Bleuse, F. Chandezon and A. Pron, *Mater. Chem. Phys.*, 2004, **84**, 10–13.
15 H.-S. Chen, B. Lo, J.-Y. Hwang, G.-Y. Chang, C.-M. Chen, S.-J. Tasi and S.-J. Jassy Wang, *J. Phys. Chem. B*, 2004, **108**, 17119–17123.
16 S. L. Cumberland, K. M. Hanif, A. Javier, G. A. Khitrov, G. F. Strouse, S. M. Woessner and C. S. Yun, *Chem. Mater.*, 2002, **14**, 1576–1584.
17 X. Wang, J. Zhuang, Q. Peng and Y. Li, *Nature*, 2005, **437**, 121–124.
18 C. L. Li, K. Nishikawa, M. Ando, H. Enomoto and N. Murase, *Colloids Surf., A*, 2007, **294**, 33–39.
19 (*a*) M. P. Pileni, *Langmuir*, 1997, **13**, 3266–3276; (*b*) J.-P. Ge, W. Chen, L.-P. Liu and Y.-D. Li, *Chem.–Eur. J.*, 2006, **12**, 6552–6558; (*c*) D. Ingert and M. P. Pileni, *Adv. Funct. Mater.*, 2001, **11**, 136–139.
20 G. N. Karanikolos, N.-L. Law, R. Mallory, A. Petrou, P. Alexandridis and T. J. Mountziaris, *Nanotechnology*, 2006, **17**, 3121–3128.
21 C. d. Mello Donegá, P. Liljeroth and D. Vanmaekelbergh, *Small*, 2005, **1**, 1152–1162.
22 C. B. Murray, D. J. Norris and M. G. Bawendi, *J. Am. Chem. Soc.*, 1993, **115**, 8706–8715.
23 W. Yu and X. Peng, *Angew. Chem., Int. Ed.*, 2002, **41**, 2368–2371.
24 H. Liu, J. S. Owen and A. P. Alivisatos, *J. Am. Chem. Soc.*, 2006, **129**, 305–312.
25 L. S. Li, N. Pradhan, Y. Wang and X. Peng, *Nano Lett.*, 2004, **4**, 2261–2264.
26 J. Park, K. An, Y. Hwang, J.-G. Park, H.-J. Noh, J.-Y. Kim, J.-H. Park, N.-M. Hang and T. Hyeon, *Nat. Mater.*, 2004, **3**, 891–895.
27 X. Wang, Q. Peng and Y. Li, *Acc. Chem. Res.*, 2007, **40**, 635–643.
28 L. Manna, D. J. Milliron, A. Meisel, E. C. Scher and A. P. Alivisatos, *Nat. Mater.*, 2003, **2**, 382–385.
29 P. D. Cozzoli, L. Manna, M. L. Curri, S. Kudera, C. Giannini, M. Striccoli and A. Agostiano, *Chem. Mater.*, 2005, **17**, 1296–1306.

30 (*a*) Y.-C. Zhu and Y. Bando, *Chem. Phys. Lett*., 2003, **377**, 367–370; (*b*) J. Hu, Y. Bando and D. Goldberg, *Small*, 2005, **1**, 95–99.
31 N. Pradhan and S. Efrima, *J. Phys. Chem. B*, 2004, **108**, 11964–11970.
32 A. B. Panda, S. Acharya and S. Efrima, *Adv. Mater*., 2005, **17**, 2471–2474.
33 T. Sugimoto, *Monodispersed Particles*, Elsevier, Amsterdam, 1st edn, 2001.
34 S.-H. Wei and A. Zunger, *Appl. Phys. Lett*., 1998, **72**, 2011–2013.
35 M. Lomascolo, A. Cretí, G. Leo, L. Vasanelli and L. Manna, *Appl. Phys. Lett*., 2003, **82**, 418–420.
36 H.-S. Chen, B. Lo, J.-Y. Hwang, G.-Y. Chang, C.-M. Chen, S.-J. Tasi and S.-J. Jassy Wang, *J. Phys. Chem. B*, 2004, **108**, 17119–17123.
37 L. P. Balet, S. A. Ivanov, A. Piryatinski, M. Achermann and V. I. Klimov, *Nano Lett*., 2004, **4**, 1485–1488.
38 X. H. Zhong, R. G. Xie, Y. Zhang, T. Basché and W. Knoll, *Chem. Mater*., 2005, **17**, 4038–4042.
39 P. Reiss, J. Bleuse and A. Pron, *Nano Lett*., 2002, **2**, 781–784.
40 Y. J. Lee, T. G. Kim and Y. M. Sung, *Nanotechnology*, 2006, **17**, 3539–3542.
41 Y. M. Sung, K. S. Park, Y. J. Lee and T. G. Kim, *J. Phys. Chem. C*, 2007, **111**, 1239–1242.
42 P. Reiss, S. Carayon, J. Bleuse and A. Pron, *Synth. Met*., 2003, **139**, 649–652.
43 D. V. Talapin, I. Mekis, S. Go1tzinger, A. Kornowski, O. Benson and H. Weller, *J. Phys. Chem. B*, 2004, **108**, 18826–18831.
44 M. Protière and P. Reiss, *Small*, 2007, **3**, 399–403.
45 (*a*) J. E. Bernard and A. Zunger, *Phys. Rev. B*, 1986, **34**, 5992–5995; (*b*) J. E. Bernard and A. Zunger, *Phys. Rev. B*, 1986, **36**, 3199–3228.
46 L. A. Swafford, L. A. Weigand, M. J. Bowers II, J. R. McBride, J. L. Rapaport, T. L. Watt, S. K. Dixit, L. C. Feldman and S. J. Rosenthal, *J. Am. Chem. Soc*., 2006, **128**, 12299–12306.
47 R. E. Bailey and S. Nie, *J. Am. Chem. Soc*., 2003, **125**, 7100–7106.
48 B. T. Kolomiets and C. M. Ling, *Sov. Phys. Solid State*, 1960, **2**, 154–156.
49 (*a*) X. Zhong, Z. Zhang, S. Liu, M. Han and W. Knoll, *J. Phys. Chem. B*, 2004, **108**, 15552–15559; (*b*) J. S. Steckel, P. Snee, S. Coe-Sullivan, J. P. Zimmer, J. E. Halpert, P. Anikeeva, L.-A. Kim, V. Bulovic and M. G. Bawendi, *Angew. Chem., Int. Ed*., 2006, **45**, 5796–5799.
50 J. K. Furdyna, *J. Appl. Phys*., 1988, **64**, R29.
51 (*a*) B. Oczkiewicz, A. Twardowski and M. Demianiuk, *Solid State Commun*., 1987, **64**, 107–111; (*b*) J. Xue, Y. Ye, F. Medina, L. Martinez, S. A. Lopez-Rivera and W. Giriat, *J. Lumin*., 1998, **78**, 173–178.
52 D. J. Norris, N. Yao, F. T. Charnock and T. A. Kennedy, *Nano Lett*., 2001, **1**, 3–7.
53 J. F. Suyver, S. F. Wuister, J. J. Kelly and A. Meijerink, *Phys. Chem. Chem. Phys*., 2000, **2**, 5445–5448.
54 N. S. Norberg, G. L. Parks, G. M. Salley and D. R. Gamelin, *J. Am. Chem. Soc*., 2006, **128**, 13195–13203.
55 S. C. Erwin, L. Zu, M. I. Haftel, A. L. Efros, T. A. Kennedy and D. J. Norris, *Nature*, 2005, **436**, 91–94.
56 N. Pradhan and X. Peng, *J. Am. Chem. Soc*., 2007, **129**, 3339–3347.
57 N. Pradhan, D. Goorskey, J. Thessing and X. Peng, *J. Am. Chem. Soc*., 2005, **127**, 17586–17587.
58 N. Pradhan, D. Battaglia, Y. Liu and X. Peng, *Nano Lett*., 2007, **7**, 312–317.
59 (*a*) W. U. Huynh, J. J. Dittmer and A. P. Alivisatos, *Science*, 2002, **295**, 2425–2427; (*b*) B. Q. Sun, H. J. Snaith, A. S. Dhoot, S. Westenhoff and N. C. Greenham, *J. Appl. Phys*., 2005, **97**, 014914.
60 Ü. Özgür, Ya. I. Alivov, C. Liu, A. Teke, M. A. Reshchikov, S. Doğan, V. Avrutin, S.-J. Cho and H. Morkoç, *J. Appl. Phys*., 2005, **98**, 041301.

